

[Title]

[Title]

Submitted in partial fulfillment of the
requirements for the degree of
Doctor of Philosophy
in the Graduate School of Arts and Sciences

COLUMBIA UNIVERSITY

2016

© 2016
Matthew D Anthony
All rights reserved

ABSTRACT

[Title]

[Author]

[Abstract Text]

Contents

Contents	i
Acknowledgements	iii
1 Dark Matter	1
1.1 Λ CDM Model	1
1.2 Evidence of Dark Matter	3
1.3 Dark Matter Candidates	9
1.4 Detecting WIMPs	12
2 Table of Contents Title	19
3 Table of Contents Title	21
Conclusion	23
Bibliography	25

Acknowledgements

[Acknowledgments]

[Dedication]

Chapter 1

Dark Matter

For nearly a century, experimental evidence has suggested that a large portion of the universe is made up of a non-luminous type of matter. While this dark matter has only been detected indirectly via its interaction with normal matter through the gravitational force, recent experiments conclude that approximately 26% of the entire energy density of the universe is comprised by dark matter.

In this chapter, I will focus on the leading dark matter model, the experimental evidence for its existence, the different candidates for particle dark matter, and the current detection methods employed in the search for particle dark matter.

1.1 Λ CDM Model

One of the guiding principles of cosmology are the assumptions that the universe is both homogeneous and isotropic at large enough scales (typically on the order 100 Mpc or 10^5 light years). Continuing with these principles and maintaining generality, we can arrive at the Robertson-Walker space-time metric

$$ds = -c^2 dt^2 + a(t)^2 \left(\frac{dr^2}{1 - kr^2} + r^2 d\Omega^2 \right) \quad (1.1)$$

Here, $a(t)$ is called the *scale factor*, an arbitrary function of time allowing for time dependent changes of the universe, and k is a constant modeling the curvature of the

1. DARK MATTER

universe. For $k = -1$, the universe is considered open, for $k = 1$, the universe is considered close, and at $k = 0$ we are left with our Euclidean (flat) universe. Note that for $a(t) = 1$ and $k = 0$ the Robertson-Walker metric reduces to the Minkowski metric.

Using this metric in combination with Einstein's equation we can derive the equations for the Friedmann-Robertson-Walker universe described by the Friedmann equations.

$$\frac{\ddot{a}}{a} = -\frac{4\pi G}{3}(\rho + 3p) \quad (1.2)$$

$$\left(\frac{\dot{a}}{a}\right)^2 = \frac{8\pi G}{3}\rho - \frac{k}{a^2} \quad (1.3)$$

We can define several useful (and commonplace) parameters to simplify the second Friedmann equation further.

Hubble Parameter: $H = \frac{\dot{a}}{a}$

Critical Density: $\rho_{crit} = \frac{3H^2}{8\pi G}$

Density Parameters: $\Omega_i = \frac{8\pi G}{3H^2}$, $\Omega_i = \frac{\rho_i}{\rho_{crit}}$

$$\Omega - 1 = \frac{k}{H^2 a^2}, \quad \Omega = \sum_i \Omega_i = \Omega_\Lambda + \Omega_{CDM} + \Omega_{Baryon} + \Omega_{Rad} \dots \quad (1.4)$$

Here the critical density is defined such that the universe is flat ($k = 0$). One can think of $\frac{\Omega_i}{\Omega}$ as what part of the total matter and energy budget a particular component makes up. The main contributors to the density of the universe are dark energy and cold dark matter hence the Λ CDM Model. Measurements of the various density parameters and other Λ CDM parameters has been a very big area of research over the last two decades and will be discussed later in this chapter.

1.2 Evidence of Dark Matter

1.2.1 Dynamical Constraints from Clusters of Galaxies

The first evidence of dark matter came from Fritz Zwicky in 1933. Zwicky used a basic application of the virial theorem on galaxies in the Coma Cluster to estimate the mass of the cluster. He then estimated the total mass based on the brightness of the cluster and found significant disagreement between the results leading him to the conclusion that “if this would be confirmed we would get the surprising result that dark matter is present in much greater amount than luminous matter.” [1]



Figure 1.1: A composite image combining an X-ray data, courtesy of Chandra, and optical data, courtesy of the Sloan Digital Sky Survey. Image credit: X-ray - NASA/CXC/MPE/J.Sanders et al, Optical - SDSS

1.2.2 Dynamical Constraints from Galactic Rotation Curves

Nearly fourty years later, stronger evidence was provided for the existence of dark matter by Vera Rubin and Kent Ford in their 1970 paper looking at the rotation curve of the Andromeda Galaxy [3]. In this paper, Rubin used the H α lines to determine

1. DARK MATTER

the orbital velocities of different stars in the galaxy. Later measurements used the 21 cm hyperfine transition line to measure orbital velocities within other galaxies [2].

From simple Newtonian arguments, one gets the following description of the orbital velocity inside a galaxy:

$$v(r) = \sqrt{\frac{GM(r)}{r}} \quad (1.5)$$

In this equation, $M(r)$ is the sum of the masses of all the gas and stars inside a given radius. Given that most of the mass from luminous matter is concentrated at the center, one would expect that at large distances from the center of the galaxy, the orbital velocity would fall off as $v \propto r^{-1/2}$.

However, what is seen differs from this simple approximation drastically. Fig. 1.2 is taken from Ref. [2] but the results are similar to what Rubin and Ford saw decades earlier: the asymptotic behavior of the orbital velocity is constant and does not show any polynomial roll-off. By isolating the contributions from measurable mass densities (such as visible matter and gas), one can get an idea of the density distribution of dark matter in a galaxy. From the figure below, one could asymptotically estimate that $M(r) \propto r$ which would imply that $\rho(r) \propto r^{-2}$. One quickly realizes that this

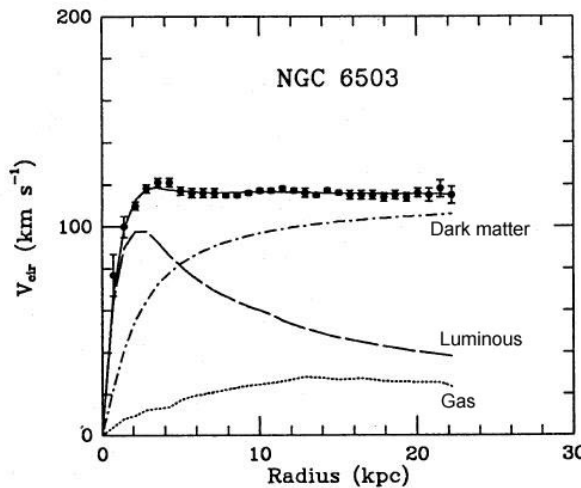


Figure 1.2: The rotation curve of the galaxy NGC 6503 broken down into individual components: visible matter (dashed), gas (dotted), and dark matter (dash dotted) [2].

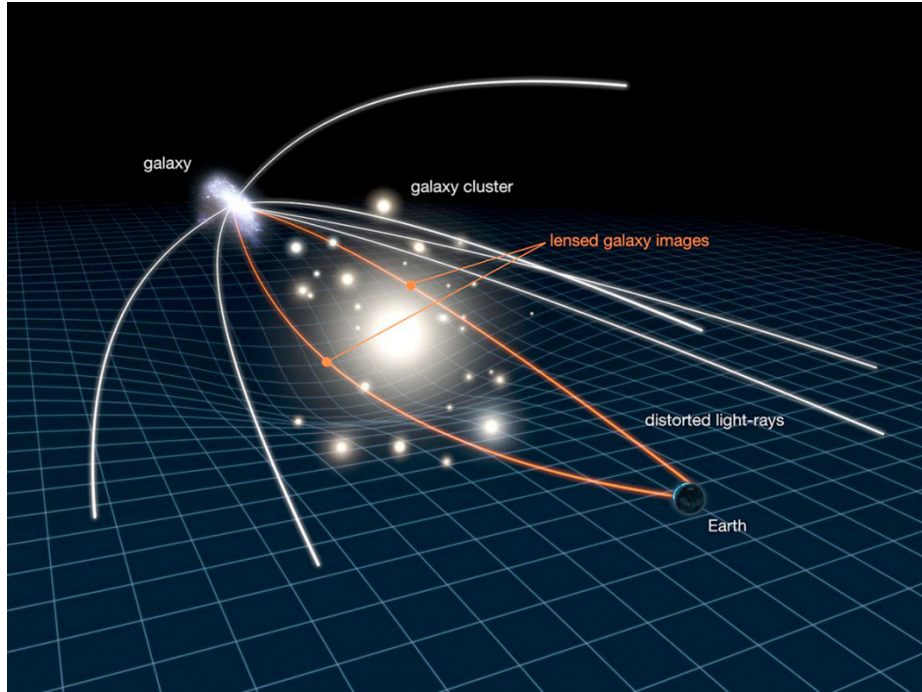


Figure 1.3: A cartoon showing the deflection of light due to the warping of spacetime caused by the presence of a massive galaxy cluster. Note that for very strong lensing, one expects multiple images of the source object and sometimes even an Einstein Ring around the lense. Image credit: NASA/ESA.

cannot be the true density since the mass of the galaxy diverges but approximates the density within an effective radius.

1.2.3 Evidence from Gravitaional Lensing

Gravitational lensing is the distortion of light coming from a source due to the warping of spacetime from the presence of large amounts of matter or energy. This effect is illustrated in Fig. 1.3 and actually captured in the form of an Einstein Cross in Fig. 1.4. In a gravitational lensing system, if we know the redshift (distance) of the source and the lense, we can estimate the gravitational field of the lensing system and hence its mass.

Mass estimation via gravitational lensing in itself is very useful for finding large discrepancies in mass from known sources and true mass (the discrepancy being attributed to dark matter). However, when combined with x-ray measurements, as

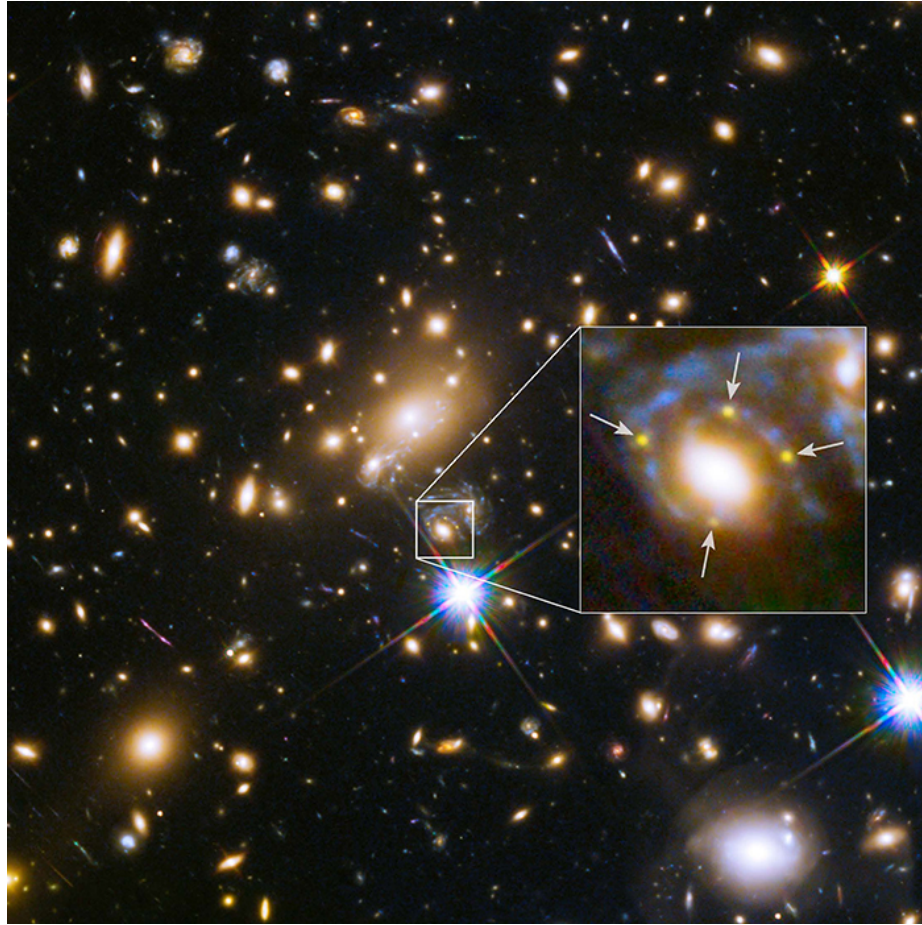


Figure 1.4: In this optical image you see the massive MACS J1149.6+2223 cluster. In the zoomed portion, you can actually see the same supernova, SN Refsdal, in four smaller images around a large galaxy within the cluster. Image credit: HST.

seen in Fig. 1.5, one gets even more interesting results. Shown in Fig. 1.5 is the Bullet Cluster (1E0657-558) which actually consists of two colliding sub-clusters. In the image on the left, one can see the infrared image from Magellan that is used, along with optical images from Hubble, to estimate the mass distribution of each galaxy cluster through gravitational lensing. In the right image, one can see the X-ray map of the Bullet Cluster from the Chandra X-ray observatory with the same mass contours: one can see that the plasma from the clusters interacts giving the cone shapes in the center. However, the mass contours largely remained centered on the individual clusters (as seen in the optical image) implying that the majority of the matter interacted minimally during the collision [4]. This implies that the majority

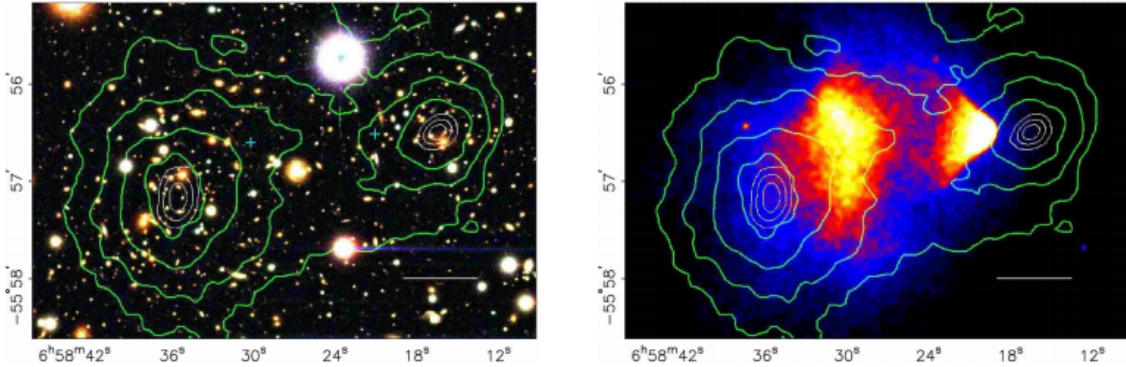


Figure 1.5: Infrared (left) and X-ray (right) maps of the Bullet Cluster (1E0657-558). While the plasma in the clusters interact during the collision of the two individual clusters, as is seen by the shockwave in the center, the majority of the mass passes right through [4].

of the matter in these clusters at least does not interact electromagnetically.

1.2.4 Evidence from the Cosmic Microwave Background

The Cosmic Microwave Background (CMB) has proved to be one of the richest discoveries in all of cosmology. Accidentally discovered in 1964 by Penzias and Wilson [5], the radiation from the CMB is almost perfectly isotropic and described by a blackbody spectrum at 2.725 K [6]. The isotropy in the CMB provides the strongest evidence to date of the Big Bang Hypothesis and helped to formulate our current picture of the early universe down to the recombination epoch, where the universe was sufficiently cool such that hydrogen could form from the free electrons and protons in turn allowing photons to travel freely through the universe.

As the CMB has been studied in more detail, cosmologists began to see that there are in fact very small temperature fluctuations on the order of $\lesssim 100 \mu K$ [7–9]. These temperature fluctuations, as seen in the 2015 measurement of the CMB by Planck satellite, are shown in Fig. 1.6. To characterize the temperature fluctuations of the entire sky, we use the spherical harmonics, $Y_{lm}(\theta, \phi)$.

$$T(\theta, \phi) = \sum_{l=0}^{\infty} \sum_{m=-l}^l a_{lm} Y_{lm}(\theta, \phi) \quad (1.6)$$

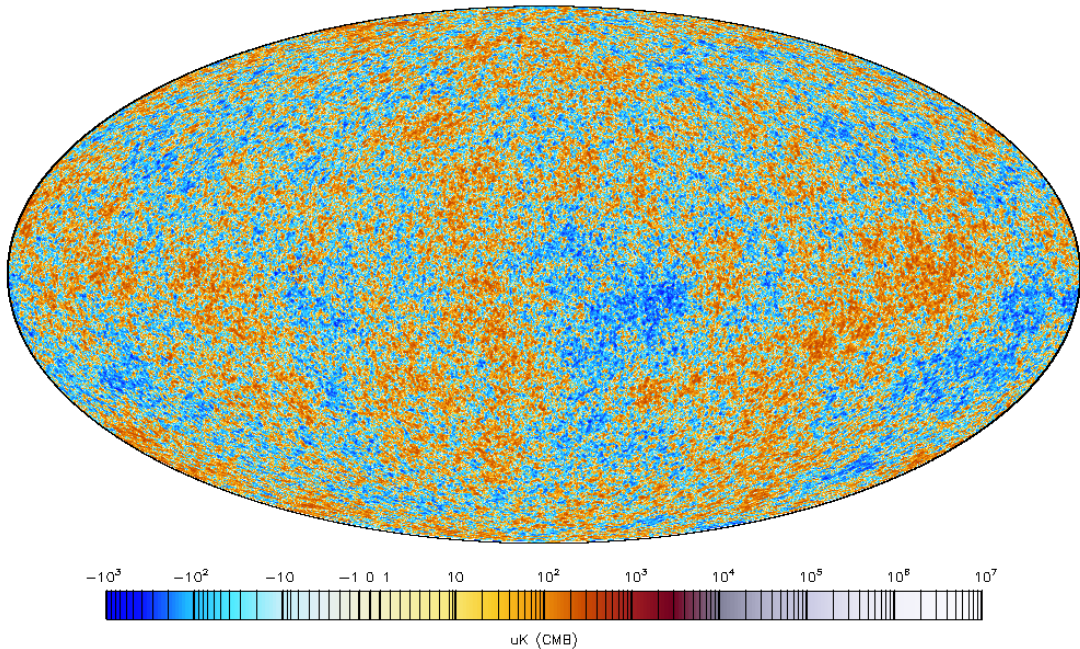


Figure 1.6: The Planck 2015 measurement of the temperature anisotropy of the CMB. Note that the largest deviations from the mean are on the order of $200\mu K$ from the 2.725 K mean (roughly 1 in 10^4). Image credit: IRSA, [7].

We assume that the distribution of a_{lm} should be described by a Gaussian distribution, as predicted by inflation, with a mean of 2.725 K for any given multipole moment l . Therefore, the only piece missing to completely describe these a_{lm} for each multiple moment is the variance of this distribution so we define $C_l \equiv \langle |a_{lm}|^2 \rangle$. These C_l form the power spectrum of the CMB and can be used to test various formation models of the universe. Planck tested the Λ CDM model described in Sec. 1.1 against their power spectrum (Fig. 1.7) and found remarkable agreement between prediction and data while constraining some of the universal constants including H_0 , Ω_Λ , Ω_{CDM} , Ω_{Baryon} , and Ω_{Rad} . It is from this fit that we find that our universe has a curvature very close to zero and therefore is flat and that our universe is comprised of roughly 68.3% dark energy, 26.8% dark matter, and 4.9% ordinary matter [7].

The Λ CDM model has been tested since its inception using N-body simulations to propagate the formation of large scale structure in the universe. While small discrepancies between simulation and observation have been found, it is clear from

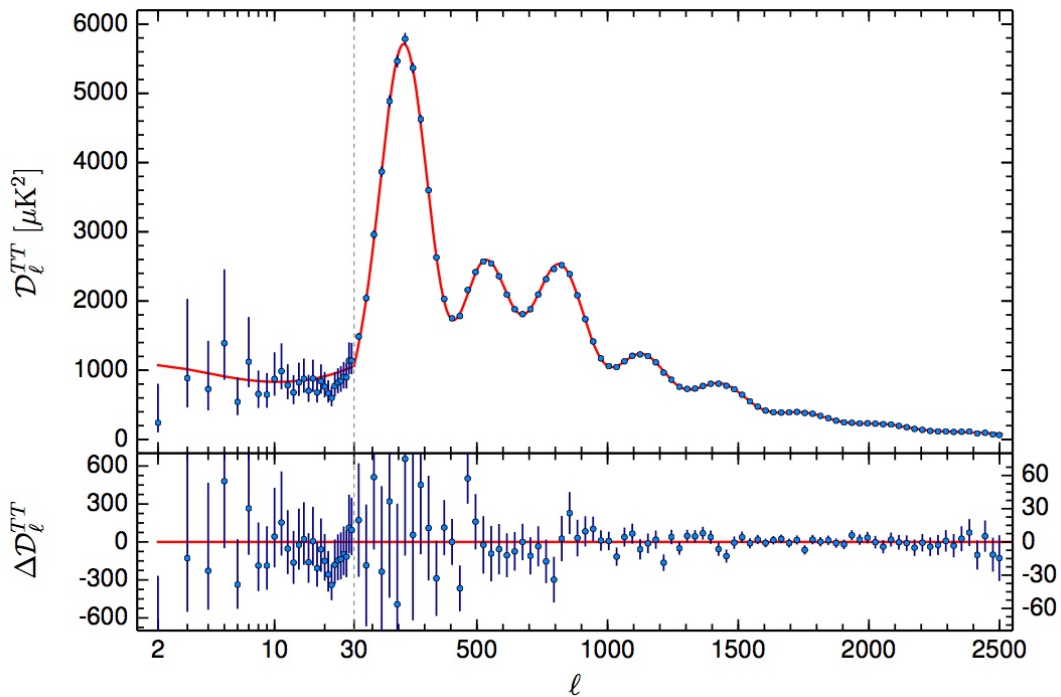


Figure 1.7: The power spectrum of the temperature anisotropies measured by Planck along with the best fit prediction from the Λ CDM model. \mathcal{D}_l^{TT} is a proxy for C_i and is defined $\mathcal{D}_l^{TT} \equiv l(l+1)C_l/2\pi$ [7].

these simulations that without cold dark matter it is extremely difficult to explain the large scale structure we see in the universe given the anisotropies of the CMB [10–12].

1.3 Dark Matter Candidates

While there is an abundance of evidence to suggest that dark matter exists, we have little evidence to suggest what this cold dark matter actually is. In this section, we will discuss two of the most popular candidates for dark matter and their physical motivations. It should be noted that the candidates discussed do not form an exhaustive list but do satisfy the most basic requirements of a dark matter candidate:

- The lifetime of the particle is much greater than the lifetime of the universe (or is stable)

1. DARK MATTER

- The particle must be electrically neutral and very weakly interacting with ordinary matter
- The particle must be able to provide the correct relic density of cold dark matter as predicted by the CMB

1.3.1 Axions

Axions are hypothetical standard model particles that are introduced via the Peccei-Quinn mechanism as a solution to the strong-CP problem, one of the largest remaining deficiencies in the standard model [13]. CP (charge and parity) symmetry violation is required to explain the imbalance of matter and antimatter in the universe (why more matter exists) and has been observed in electroweak theory in a wide variety of measurements [14–18]. CP violation has never been observed in quantum chromodynamics even though there are natural terms in the QCD Lagrangian that would allow it. Therefore, this term in the Lagrangian, must be fine-tuned to exactly zero, hence the strong-CP problem. The axion introduced by Peccei-Quinn theory replaces this term with a field and gives the Lagrangian natural CP symmetry.

While the discovery of the axion would solve one of the largest problems of standard model, it also has the potential to solve one of the largest open mysteries of cosmology by making up at least a part of the cold dark matter density of the universe. Even though the axion is expected to have a very small mass ($10^{-6} - 10^{-2} \text{ eV}$) it could still be produced cosmologically such that the large scale structure that we observe in the universe today is explained and we arrive at the CDM density estimated by Planck [19].

There are a number of experiments that can provide information about axions, both directly and indirectly. The mass range of axions, is essentially restricted from cosmological evidence from the CMB and stellar evolution. Simultaneously, cavity microwave experiments such as ADMX [20] and NMR based searches such as CASPeR [21] try to directly detect these low mass CDM candidates.

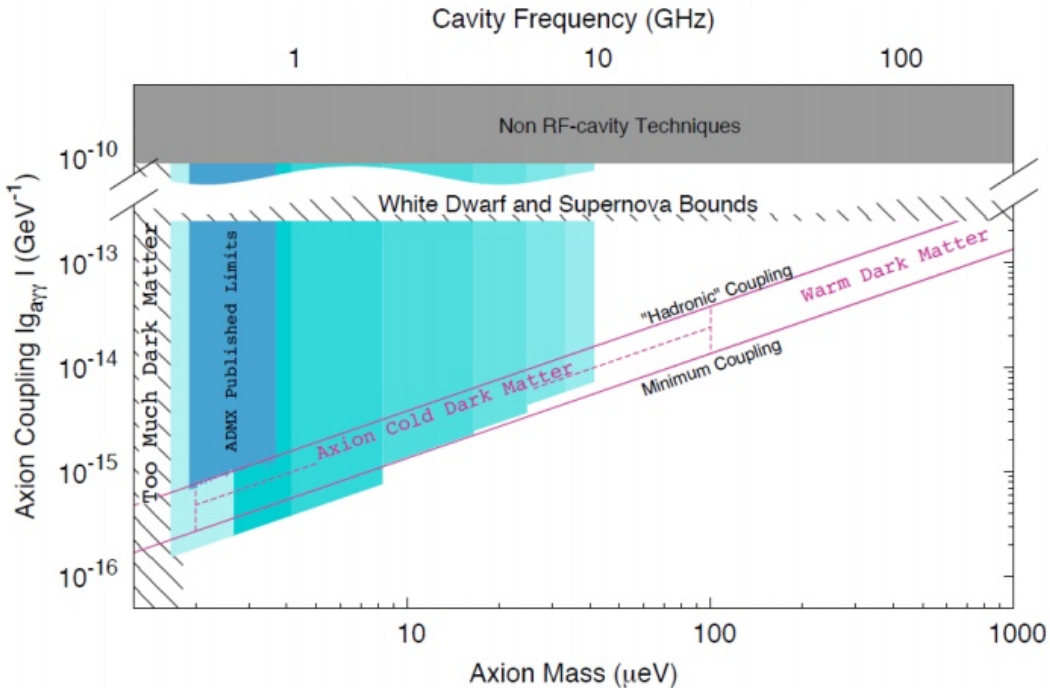


Figure 1.8: The projected sensitivity of the ADMX Generation 2 axion search. Note that strong cosmological constraints are placed on the mass range and the axion coupling is also constrained by the mass. The ADMX collaboration predicts that the searches shown will be completed by 2022 [20].

1.3.2 WIMPs

Weakly interacting massive particles (WIMPs), which will be the focus of the remainder of this work, have proven to be the most popular dark matter candidate historically. WIMPs not only satisfy the basic criteria listed at the beginning of this section but additionally they have what is referred to as the “WIMP Miracle” in their favor. In the early stages of the universe, the temperature and density were so large that all particles were in a state of chemical equilibrium. A dark matter particle could annihilate by colliding with its anti-partner to form any type of particle vice versa. As time passed, however, the universe expanded and cooled making it more unlikely for these dark matter particles to be created or destroyed. Using this thermal equilibrium model alongside the Λ CDM model, one can infer that the CDM density in the universe today is approximately given by [22, 23]

$$\Omega_{CDM} h^2 \approx \frac{3 \times 10^{-27} \text{cm}^3 \text{s}^{-1}}{\langle \sigma_{ann} v \rangle} \quad (1.7)$$

where $\langle \sigma_{ann} v \rangle$ is thermally averaged annihilation cross-section of cold dark matter. Incredibly enough, if we assume that cold dark matter has properties such as cross-section and mass on the weak scale, we find that $\Omega_{CDM} h^2 \approx 0.1$, which is in agreement with cosmological constraints.

In addition to WIMPs agreeing with cosmological evidence, several WIMP-like particles having masses on the order of 100 GeV with very long lifetimes naturally fall out of extensions of the standard model, such as supersymmetry.

1.4 Detecting WIMPs

Over the last few decades there has been an enormous concerted effort to detect WIMPs. This effort has been focused in three general approaches: indirect detection, collider detection, and direct detection. Fig. 1.9 shows the idea behind these approaches:

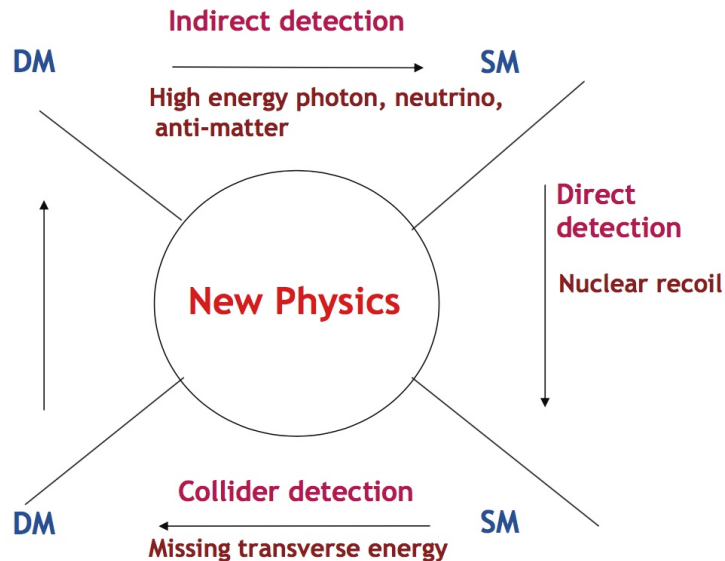


Figure 1.9: The three general approaches to WIMP detection: indirect detection, collider detection, and direct detection. Image credit: [24].

- Direct detection looks for the scattering of WIMPs with ordinary matter
- Indirect detection looks for the annihilation of WIMPs in our galaxy into ordinary matter
- Collider detection is an attempt at creating WIMPs by colliding ordinary matter

1.4.1 Indirect Detection

As we know from previous sections, WIMPs, if they make up all (or some) of the dark matter in the universe, must reside in galaxies to explain the odd behavior of rotation curves and the mass discrepancies. Given the observational evidence, simulations have been created that can predict both the distribution of dark matter within our own and other galaxies [25, 26] and the density of dark matter in our own solar system (roughly $0.2 - 0.4 \frac{GeV}{cm^3}$ [27]). Indirect detection experiments look at high density regions of dark matter halos, such as in or around the Milky Way center and dwarf galaxies, to search for annihilations of WIMPs into detectable particles.

The goal of indirect detection is to capture a dark matter annihilation by observing its byproducts. In the ideal case, two dark matter particles would annihilate and create two photons with energies equal to the mass of the dark matter particle. Even though this would be the “smoking gun” evidence of dark matter, most of the standard model extension WIMPs predict that this would be highly suppressed. Instead, these indirect experiments are more likely to observe the annihilation of WIMPs into other particles which in turn will produce photons [24].

A major difficulty in indirect detection experiments is distinguishing potential signals from normal astrophysical processes. Since areas of high dark matter density are also typically areas of high astrophysical activity it becomes difficult to separate potential dark matter signals from potentially new astrophysics [28]. However, in recent years, astrophysicists have started turning their telescopes towards dwarf galaxies, which are dark matter dominated but have negligible astrophysical backgrounds [29].

1.4.2 Collider Detection

The main idea behind collider detection is that since the WIMP is expected to have a mass on the order of $1 - 10^3$ GeV is that we can create it in particle accelerators. Of course, detectors at particle accelerators are not designed to detect dark matter directly so when searching for WIMPs physicists must actually search for missing transverse energy (MET) in a collision. detect it via the missing transverse energy (MET). The MET can be reconstructed by observing the outgoing particles and jets in a collision based on momentum conservation. This reconstruction is shown in Fig. 1.10. Ultimately, this MET can be used to determine the mass and the new physics processes of the WIMP [24].

One important note is that while we can potentially “see” WIMPs in detectors at colliders, it is impossible to be certain that this WIMP is what makes up the majority of the matter in the universe. The same signal would need to be seen in indirect and direct searches as well to make such a confirmation [30].

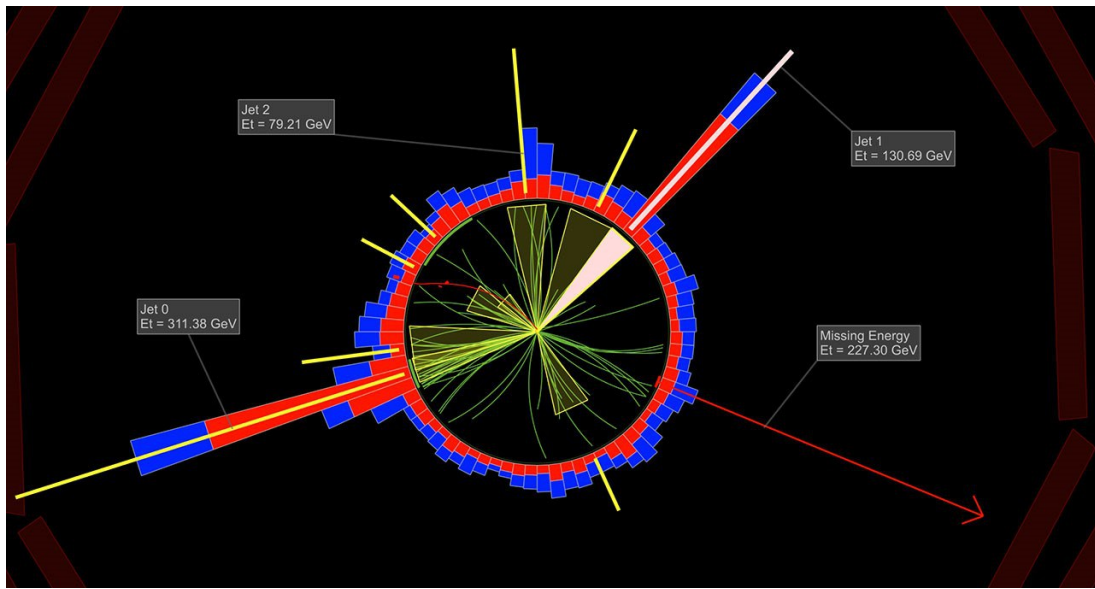


Figure 1.10: An image of a potential WIMP event in the CMS detector at CERN. If a WIMP is present in a collision, momentum would not be conserved after all jets and particles have been accounted for in the collision. Here we can see that after the three jets are reconstructed that there is still a large MET that could potentially be attributed to a WIMP. Image courtesy: Matevz Tadel, UC San Diego/CMS.

1.4.3 Direct Detection

In purely theoretical terms, any detector that is sensitive to a potential WIMP interaction could be considered a direct detection dark matter search. At the same time, to try and detect a dark matter signal from your NaI detector in your lab would be preposterous (unless your detector is 250 kg and located deep underground!), the reason being that any of the rare dark matter signals would be drowned out by the countless background events you would also to detect. This is why direct detection experiments are typically built deep underground with shielding and low radiation materials and take great care to understand their background as well as they possibly can: if WIMPs are scattering in the detector they want to be able to know.

The goal of direct detection experiments is to detect the scatter of WIMPs off of standard model particles. As mentioned, since these scatters should be extremely rare, it is essential to have the background of the detector used be as low as possible. As a simple example, consider two otherwise identical experiments who both have measured their backgrounds perfectly: experiment A expects a single background event per year while experiment B expects 1,000 background events per year. In the case that both detectors see an excess of ten events in a given year over their background, it should be clear that experiment A can make a very strong claim that they have seen WIMP scatterings where as experiment B cannot since this excess could very well be a fluctuation from their expected background.

It cannot be emphasized strongly enough how crucial the understanding of background is for direct detection experiments. Returning to the above example, imagine experiment A missed a source of background in their estimate and that their true expected background rate is ten events per year, not one. If they saw the same eleven events as before, they might claim a discovery even though the eleven events are very likely to be a statistical fluctuation of the background.

The most basic models describing WIMPs predict that they are most likely to interact with atomic nuclei (although some predict leptonic interactions [31]). This assumption, along with cosmological evidence that WIMPs are non-relativistic, sur-

prisingly gives way to a fairly straight-forward derivation of the rate of scattering that one could expect for different nuclei, and therefore a complete detector, assuming a given scattering cross-section and mass for the WIMP. For a complete derivation one should refer to Ref. [22] and Ref. [32].

It can be shown that the differential scattering rate is given by [33]

$$\frac{dR}{dE}(E) = \frac{\rho_0}{m_\chi m_A} \int_{v_{\min}(E)}^{v_{\text{esc}}} v f(v) \frac{d\sigma}{dE}(E, v) dv \quad (1.8)$$

where ρ_0 is the local dark matter density, m_χ is the mass of the WIMP, m_A is the mass of the target nucleus, $f(v)$ is the velocity distribution of dark matter locally, v_{\min} is the minimum velocity that can produce a recoil of energy E , v_{esc} is the maximum velocity in which WIMPs are still gravitationally bound to the galactic halo, and $\frac{d\sigma}{dE}$ is the differential cross-section of WIMP-nucleon scattering.

As discussed in Sec. 1.4.1, N-body simulations give us a prediction of roughly $0.2 - 0.4 \frac{\text{GeV}}{\text{cm}^3}$ for the local dark matter density [27]. We will use the standard halo model (SHM), which is standard for dark matter experiments, such that the velocity of WIMPs in the halo follows a Maxwell-Boltzmann distribution. The minimum velocity of a WIMP to transfer an energy E to a nucleus, v_{\min} , is found kinematically to be

$$v_{\min} = \sqrt{\frac{m_A E}{2\mu^2}}, \quad \mu = \frac{m_A m_\chi}{m_A + m_\chi} \quad (1.9)$$

while astrophysical measurements of the Milky Way estimate the local escape velocity to be $v_{\text{esc}} = 533^{+54}_{-41} \text{ km s}^{-1}$ [34]. It is worth noting that while the Maxwell-Boltzmann distribution is the standard, other models of the velocity distribution exist [35].

The particle physics of the WIMPs comes in at the differential cross-section. The most basic WIMP models predict two potential interactions: a spin-independent or spin-dependent. Focusing on the former, the differential cross-section is given by

$$\frac{d\sigma}{dE}(E, v) = \frac{m_A}{2\mu^2 v^2} \sigma_0 F(E)^2 \quad (1.10)$$

where $F(E)$ is nuclear form factor. The nuclear form factor is the Fourier transform

of the ground state mass density and is used to reduce to correct the zero-momentum transfer cross-section in the case of a momentum transfer. The nuclear form factor can be approximated by

$$F(q) = \frac{3j_1(qR_0)}{qR_0} e^{\frac{-(qs)^2}{2}}, \quad q = \sqrt{2m_A E}, \quad R_0^2 = \left(1.2A^{\frac{1}{3}} \text{ fm}\right)^2 - 5s^2 \quad (1.11)$$

where q is the momentum transfer in the scatter, R_0 is the approximate nuclear radius, s is the approximate thickness of the nucleus (roughly 1 fm), and j_1 is the spherical Bessel function of the first kind [36].

We can reduce σ_0 , the cross-section of an interaction with zero momentum transfer, by accounting for the coupling to the individual nucleons in the following way

$$\sigma_0 = \frac{(Zf_p + (A-Z)f_n)^2}{f_p^2} \frac{\mu^2}{\mu_{\chi p}^2} \sigma_p \quad (1.12)$$

In this equation, f_p and f_n are the WIMP couplings to the proton and neutron, respectively, $\mu_{\chi p}$ is the reduced mass of the WIMP-proton system, and σ_p is the spin-independent cross-section of the WIMP with the proton. We approximate that $f_p \approx f_n$ which allows us to simplify to

$$\sigma_0 \approx A^2 \frac{\mu^2}{\mu_{\chi p}^2} \sigma_p \quad (1.13)$$

All of this can be combined such that we are only dependent on two variables: the mass of the WIMP and its cross-section with a proton.

$$\frac{dR}{dE} = \frac{\rho_0 A^2 \sigma_p}{2m_\chi \mu_{\chi p}} F(E)^2 \int_{v_{\min}(E)}^{v_{\text{esc}}} \frac{f(v)}{v} dv \quad (1.14)$$

Chapter 2

Title of Chapter 2

Here you can write some introductory remarks about your chapter. I like to give each sentence its own line.

When you need a new paragraph, just skip an extra line.

New Section

By using the asterisk to start a new section, I keep the section from appearing in the table of contents. If you want your sections to be numbered and to appear in the table of contents, remove the asterisk.

Chapter 3

Title of Chapter 3

Here you can write some introductory remarks about your chapter. I like to give each sentence its own line.

When you need a new paragraph, just skip an extra line.

New Section

By using the asterisk to start a new section, I keep the section from appearing in the table of contents. If you want your sections to be numbered and to appear in the table of contents, remove the asterisk.

Conclusion

Here you can write some introductory remarks about your chapter. I like to give each sentence its own line.

When you need a new paragraph, just skip an extra line.

New Section

By using the asterisk to start a new section, I keep the section from appearing in the table of contents. If you want your sections to be numbered and to appear in the table of contents, remove the asterisk.

Bibliography

- [1] F. Zwicky, “The redshift of extragalactic nebulae,” *Helv. Phys. Acta*, vol. 6, p. 110, 1933.
- [2] K. Begeman, A. Broeils, and R. Sanders, “Extended rotation curves of spiral galaxies: dark haloes and modified dynamics,” *Monthly Notices of the Royal Astronomical Society*, vol. 249, no. 3, pp. 523–537, 1991.
- [3] V. C. Rubin and W. K. Ford Jr, “Rotation of the andromeda nebula from a spectroscopic survey of emission regions,” *The Astrophysical Journal*, vol. 159, p. 379, 1970.
- [4] D. Clowe, M. Bradač, A. H. Gonzalez, M. Markevitch, S. W. Randall, C. Jones, and D. Zaritsky, “A direct empirical proof of the existence of dark matter,” *The Astrophysical Journal Letters*, vol. 648, no. 2, p. L109, 2006.
- [5] A. A. Penzias and R. W. Wilson, “A measurement of excess antenna temperature at 4080 mc/s.,” *The Astrophysical Journal*, vol. 142, pp. 419–421, 1965.
- [6] D. Fixsen, E. Cheng, J. Gales, J. C. Mather, R. Shafer, and E. Wright, “The cosmic microwave background spectrum from the full cobe* firas data set,” *The Astrophysical Journal*, vol. 473, no. 2, p. 576, 1996.
- [7] P. A. Ade, V Salvatelli, V Stolyarov, F. Desert, J Knoche, M Giard, X Dupac, M Liguori, S Matarrese, Z Huang, *et al.*, “Planck 2015 results. xiii. cosmological parameters,” *Astron. Astrophys.*, vol. 594, no. arXiv: 1502.01589, A13, 2015.
- [8] C. L. Bennett, A. J. Banday, K. M. Górski, G Hinshaw, P Jackson, P Keegstra, A Kogut, G. F. Smoot, D. T. Wilkinson, and E. L. Wright, “Four-year cobe* dmr cosmic microwave background observations: maps and basic results,” *The Astrophysical Journal Letters*, vol. 464, no. 1, p. L1, 1996.
- [9] E. Komatsu, K. Smith, J Dunkley, C. Bennett, B Gold, G Hinshaw, N Jarosik, D Larson, M. Nolta, L Page, *et al.*, “Seven-year wilkinson microwave anisotropy probe (wmap*) observations: cosmological interpretation,” *The Astrophysical Journal Supplement Series*, vol. 192, no. 2, p. 18, 2011.

BIBLIOGRAPHY

- [10] J. F. Navarro, “The structure of cold dark matter halos,” in *Symposium-international astronomical union*, Cambridge University Press, vol. 171, 1996, pp. 255–258.
- [11] V. Springel, C. S. Frenk, and S. D. White, “The large-scale structure of the universe,” *arXiv preprint astro-ph/0604561*, 2006.
- [12] M. Vogelsberger, S. Genel, V. Springel, P. Torrey, D. Sijacki, D. Xu, G. Snyder, D. Nelson, and L. Hernquist, “Introducing the *illustris* project: simulating the coevolution of dark and visible matter in the universe,” *Monthly Notices of the Royal Astronomical Society*, pp. 1518–1547, 2014.
- [13] R. D. Peccei and H. R. Quinn, “Cp conservation in the presence of pseudoparticles,” *Physical Review Letters*, vol. 38, no. 25, p. 1440, 1977.
- [14] A Alavi-Harati, I. Albuquerque, T Alexopoulos, M Arenton, K Arisaka, S Averitte, A. Barker, L. Bellantoni, A Bellavance, J Belz, *et al.*, “Observation of direct CP violation in $K_{S,L} \rightarrow \pi\pi$ decays,” *Physical Review Letters*, vol. 83, no. 1, p. 22, 1999.
- [15] V Fanti, A Lai, D Marras, L Musa, A. Bevan, T. Gershon, B Hay, R. Moore, K. Moore, D. Munday, *et al.*, “A new measurement of direct CP violation in two pion decays of the neutral kaon,” *Physics Letters B*, vol. 465, no. 1, pp. 335–348, 1999.
- [16] B. Aubert, D Boutigny, I De Bonis, J.-M. Gaillard, A Jeremie, Y Karyotakis, J. Lees, P Robbe, V Tisserand, A Palano, *et al.*, “Measurement of CP-violating asymmetries in B^0 decays to CP eigenstates,” *Physical Review Letters*, vol. 86, no. 12, p. 2515, 2001.
- [17] K. Abe, R Abe, I Adachi, B. S. Ahn, H Aihara, M Akatsu, G Alimonti, K Asai, M Asai, Y Asano, *et al.*, “Observation of large CP violation in the neutral B meson system,” *Physical Review Letters*, vol. 87, no. 9, p. 091802, 2001.
- [18] R Aaij, C. A. Beteta, B Adeua, M Adinolfi, C Adrover, A Affolder, Z Ajaltouni, J Albrecht, F Alessio, M Alexander, *et al.*, “First observation of CP violation in the decays of B_s^0 mesons,” *Physical review letters*, vol. 110, no. 22, p. 221601, 2013.
- [19] P. W. Graham, I. G. Irastorza, S. K. Lamoreaux, A. Lindner, and K. A. van Bibber, “Experimental searches for the axion and axion-like particles,” *Annual Review of Nuclear and Particle Science*, vol. 65, pp. 485–514, 2015.
- [20] I. Stern, “Admx status,” *arXiv preprint arXiv:1612.08296*, 2016.

- [21] A. Garcon, D. Aybas, J. W. Blanchard, G. Centers, N. L. Figueroa, P. Graham, D. F. J. Kimball, S. Rajendran, M. G. Sendra, A. O. Sushkov, *et al.*, “Searching for dark matter with nuclear magnetic resonance: the cosmic axion spin precession experiment,” *arXiv preprint arXiv:1707.05312*, 2017.
- [22] G. Jungman, M. Kamionkowski, and K. Griest, “Supersymmetric dark matter,” *Physics Reports*, vol. 267, no. 5-6, pp. 195–373, 1996.
- [23] G. Bertone, *Particle dark matter: Observations, models and searches*. Cambridge University Press, 2010.
- [24] X.-J. Bi, P.-F. Yin, and Q. Yuan, “Status of dark matter detection,” *Frontiers of Physics*, vol. 8, no. 6, pp. 794–827, 2013.
- [25] J. Stadel, D. Potter, B. Moore, J. Diemand, P. Madau, M. Zemp, M. Kuhlen, and V. Quilis, “Quantifying the heart of darkness with ghalo—a multibillion particle simulation of a galactic halo,” *Monthly Notices of the Royal Astronomical Society: Letters*, vol. 398, no. 1, pp. L21–L25, 2009.
- [26] A. V. Macciò, A. A. Dutton, F. C. Van Den Bosch, B. Moore, D. Potter, and J. Stadel, “Concentration, spin and shape of dark matter haloes: scatter and the dependence on mass and environment,” *Monthly Notices of the Royal Astronomical Society*, vol. 378, no. 1, pp. 55–71, 2007.
- [27] J. Read, “The local dark matter density,” *Journal of Physics G: Nuclear and Particle Physics*, vol. 41, no. 6, p. 063101, 2014.
- [28] B. Zitzer *et al.*, “Search for dark matter from dwarf galaxies using veritas,” *arXiv preprint arXiv:1509.01105*, 2015.
- [29] J. Conrad, “Indirect detection of wimp dark matter: a compact review,” *arXiv preprint arXiv:1411.1925*, 2014.
- [30] F. S. Queiroz, “Dark matter overview: collider, direct and indirect detection searches,” *arXiv preprint arXiv:1605.08788*, 2016.
- [31] J. Kopp, V. Niro, T. Schwetz, and J. Zupan, “Dama/libra data and leptонically interacting dark matter,” *Physical Review D*, vol. 80, no. 8, p. 083502, 2009.
- [32] J. Lewin and P. Smith, “Review of mathematics, numerical factors, and corrections for dark matter experiments based on elastic nuclear recoil,” *Astroparticle Physics*, vol. 6, no. 1, pp. 87–112, 1996.

BIBLIOGRAPHY

- [33] T. M. Undagoitia and L. Rauch, “Dark matter direct-detection experiments,” *Journal of Physics G: Nuclear and Particle Physics*, vol. 43, no. 1, p. 013 001, 2015.
- [34] T. Piffl, C. Scannapieco, J. Binney, M. Steinmetz, R.-D. Scholz, M. E. Williams, R. S. De Jong, G. Kordopatis, G. Matijević, O. Bienaymé, *et al.*, “The rave survey: the galactic escape speed and the mass of the milky way,” *Astronomy & Astrophysics*, vol. 562, A91, 2014.
- [35] M. Kuhlen, N. Weiner, J. Diemand, P. Madau, B. Moore, D. Potter, J. Stadel, and M. Zemp, “Dark matter direct detection with non-maxwellian velocity structure,” *Journal of Cosmology and Astroparticle Physics*, vol. 2010, no. 02, p. 030, 2010.
- [36] J Engel, “Nuclear form factors for the scattering of weakly interacting massive particles,” *Physics Letters B*, vol. 264, no. 1-2, pp. 114–119, 1991.